Polymer Degradation and Stability 203 (2022) 110052

Contents lists available at ScienceDirect

Polymer Degradation and Stability

journal homepage: www.journals.elsevier.com/polymer-degradation-and-stability

# Water boosts reactive toughening of PET

Ferenc Ronkay [a,b], Béla Molnár [a], Edina Szabó [c], György Marosi [c], Katalin Bocz [c,*]

[a] Imsys Ltd, Material Testing Laboratory, Mozaik Street 14/A., H-1033, Budapest, Hungary
[b] Department of Polymer Engineering, Faculty of Mechanical Engineering, Budapest University of Technology and Economics, Műegyetem rkp. 3., H-1111, Budapest, Hungary
[c] Department of Organic Chemistry and Technology, Faculty of Chemical Technology and Biotechnology, Budapest University of Technology and Economics, Műegyetem rkp. 3., H-1111, Budapest, Hungary

ARTICLE INFO

*Keywords:*
Poly(ethylene terephthalate)
Recycling
Extrusion
Degradation
Reactive toughening, Impact behaviour

ABSTRACT

During melt-processing, the molecular weight of poly(ethylene terephthalate) PET, being prone to hydrolytic degradation, decreases proportionally with its initial moisture content. Therefore, to avoid undesired deterioration of the physical and mechanical properties, PET granules or recyclates are generally dried (the residual moisture must be generally lower than 500 ppm) just prior to melt-processing. In this research, in contrast to the general practice, PET granules with increasing moisture content in the range of 30-3520 ppm, as conditioned in a climate chamber, were melt blended with a constant amount (13%) of ethylene-butyl acrylate-glycidyl methacrylate (EBA-GMA) type reactive terpolymer by twin screw extrusion. It was found that moisture boosts the reactive toughening process, and consequently, the notched Izod impact strength increases by up to 600%. Notched impact strength higher than 50 kJ/m$^2$ was reached only by using PET with optimal (1710 ppm) moisture level instead of fully dried granules, as starting material. It is also noteworthy that the tensile strength and stiffness of the blends showed little variation over the examined moisture content range. Scanning electron microscopic analyses show that the size of the dispersed phase decreases continuously with the increasing initial moisture content of PET, which is explained by the increasingly effective interfacial compatibilisation with the terpolymer. Compatibilisation reactions are accelerated by the low-molecular-weight PET chains of increased reactivity that are formed *in situ* in the presence of moisture during melt-processing. The observed phenomenon can be advantageously utilized for upgrading recycling technology.

## 1. Introduction

During thermomechanical processing of poly(ethylene terephthalate) (PET), degradation unavoidably occurs, which leads to a decrease in the molecular weight of the polymer [1–3]. It is especially relevant for recycling, which is a clearly recognized work to do [4–7]. Despite careful sorting and cleaning, even the selectively collected plastic waste may suffer from deterioration due to the stress of reprocessing [8,9].

The degree of degradation is affected by the technical parameters of reprocessing: temperature; processing rate (e.g. extruder type, screw speed); residence time; contaminants (e.g. poly(vinyl chloride) (PVC), adhesive residues); the initial molecular weight; initial carboxyl end group content; and the moisture content of the material [10–13]. The latter is usually controlled by pre-drying of the PET, as even a water content of 50 ppm causes detectable degradation when processed at 280°C [14]. Hydrolytic degradation may occur just above the glass transition temperature ($T_g$) [15], but the rate of chain cleavage is enhanced with increasing temperature and humidity. At higher moisture contents, hydrolytic degradation (Fig. 1) is almost exclusively responsible for the decrease in molecular weight, while the contribution of thermal and thermo-oxidative degradation is negligible [14].

The highly amorphous PET can be considered as a pseudo-ductile polymer, which during deformation tends to fail by yielding, accompanied with high crack initiation energy (high unnotched toughness) and low crack propagation energy (low notched toughness) [17]. The brittle/ductile behavior of polymer glasses is controlled by two chain parameters: “entanglement density” and “characteristic ratio” of the chain, which is a measure of the intrinsic flexibility and rigidity of a coiled chain. Supertoughness can only be obtained when the molecular weight is at least seven times the entanglement molecular weight ($M_e$), which can be defined as the molecular weight of an entanglement strand

* Corresponding author.
*E-mail address:* bocz.katalin@vbk.bme.hu (K. Bocz).

https://doi.org/10.1016/j.polymdegradstab.2022.110052
Received 5 May 2022; Received in revised form 21 June 2022; Accepted 27 June 2022
Available online 9 July 2022

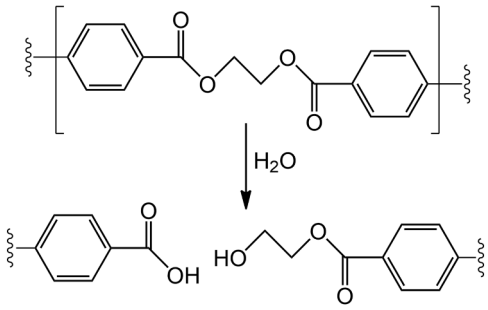


**Fig. 1.** Schematic hydrolysis reaction responsible for the reduction of molecular weight during the reprocessing of PET [16].

between two adjacent entanglement junctions along a chain [18]. For PET, there are several data in the literature for $M_e$ between 1170-1630 g/mol [19–21]. Martinez et al. [22] characterized the ductility of PET samples of different average molecular weights based on their elongation at break values. They found that this characteristic decreased abruptly at the viscosity molecular weight $M_V$ = 8300 g/mol (intrinsic viscosity *IV* = 0.37 dl/g), this is below the critical level needed to maintain an entanglement network in the solid state. Wu et al. [23] showed a drastic drop in impact strength at the *IV* value of 0.65 dl/g for PET processed with different technologies.

A common method to compensate the reduction of impact strength in the case of recycled PET is rubber toughening [24–29], which should impart greater ductility, improved crack resistance, and higher impact strength [30,31]. According to this method, the matrix polymer is blended with a rubber phase, which increases the matrix polymer yielding behaviour. At constant rubber content, the brittleness/ductility transition depends on the size of the dispersed phase. Assuming identical interfacial adhesion, this transition occurs at a critical rubber particle diameter, which corresponds to a certain surface-to-surface interparticle thickness (also termed the matrix ligament thickness). At the critical surface-to-surface ratio, the dispersed rubber particles form an infinitive interconnected network of stress volumes [32]. The critical surface-to-surface ratio is related to the characteristic ratio of the chain, so the optimum rubber phase morphology for toughening correlates with the chain parameters of the matrix polymer phase. The value depends on rate, temperature, loading mode, internal stress, and others. For PET (taking the characteristic ratio of the chain to 4.2 [19]), the critical matrix ligament thickness is about 0.5 μm [17].

Using reactive rubbers is an effective strategy to improve interfacial adhesion between the polymer matrix and the rubber phase [33,34]. During blending, the active groups in the reactive rubber react with the polar groups of the thermoplastic polymer (in the case of PET with the terminal hydroxyl or carboxyl groups) and *in situ* graft copolymers are formed at the interfaces of phases [31].

During melt mixing at high (> 240°C) processing temperatures, a crosslinking process that competes with compatibilisation may also occur in the elastomeric phase containing glycidyl methacrylate (GMA) [35]. Crosslinking can only begin upon contact with the matrix polymer, as the absence of hydroxyl groups in the rubber phase alone inhibits this process. All this has a significant effect on the morphology, as it affects the viscosity and distribution of the elastomeric phase, and the rubber particles become more elastic and less deformable. Consequently, crosslinked structure induces the formation of non-spherical shape and rough interface of the dispersed elastomeric particles.

Loyens and Groeninckx [35] investigated the effect of the molecular weight of the PET matrix on the impact behavior of PET / (EPR / E-GMA8) blends containing ethylene-co-propylene rubber (EPR) and a copolymer of ethylene and 8 wt% glycidyl methacrylate (E-GMA8). The impact strength of the blends was found to increase with the matrix molar mass, which was explained primarily by the improved phase morphology, i.e. decreased particle size of the rubber phase and decreased interparticle distance. Below the critical interparticle distance, however, the impact strength was found to be independent of the matrix molar mass.

In our previous research study [27], we have shown that the toughening efficiency of the ethylene–butyl acrylate glycidyl-methacrylate (EBA-GMA) type reactive terpolymer in PET is highly dependent on the molecular weight of the polymer matrix used. The use of recycled PET matrix, due to the larger number of reactive functional end groups and increased mobility of the reduced molecular weight chains, multiplies the notched Izod impact strength compared to that of the original PET matrix with identical EBA-GMA content. Toughening Enhancer Interphase (TEI) was defined which is formed from the shorter chain macromolecules of recycled PET reacted with the EBA-GMA phase. Using materials with different molecular weights and systematically altered EBA-GMA contents, we demonstrated that the simultaneous compatibilisation and fragmentation of the rubber particles are of key importance in the creation of large interfaces and successful toughening.

In the present research, we propose that the highly reactive short-chain fraction, that is necessitated for creating the TEI and thus achieving outstanding impact resistance at noticeably reduced terpolymer content, can be formed *in situ* during melt processing through the accelerated hydrolytic degradation of PET in the presence of controlled amount of moisture. In this study, the effect of the initial moisture content of PET is investigated on the compatibilisation and crosslinking reactions taking place during melt blending of the PET/EBA-GMA system and indirectly on the impact resistance of the obtained product.

## 2. Materials and methods

### 2.1. Materials

NeoPET 80 (Neo Group, Lithuania) type PET granules with an IV of 0.80 ± 0.02 dl/g were used as starting material ($M_w$ = 27,400; $M_n$ = 10100; PDI = 2.71 as measured by gel permeation chromatography (GPC) [36]). The mean diameter of the spherical granules is 2.7 ± 0.3 mm. The crystallinity of the used granules was 40 ± 3% as measured by differential scanning calorimetry (DSC).

Elvaloy PTW (DuPont, USA) type EBA-GMA with 5.25% GMA content and $T_m$ = 72°C was used as a reactive toughening agent.

### 2.2. Methods

#### 2.2.1. Sample preparation

The moisture content of the PET granule was set using a C-70/350 (CTS, Germany) climate chamber with different residence times at 23°C / 80% relative humidity (RH). Prior to the procedure, the granules were dried at 160°C to equilibrium water content (approx. 30 ppm). PET granules with set moisture content were then compounded with a constant 13% EBA-GMA ratio. Namely, based on our previous study [27], at this EBA-GMA content, the notched Izod impact strength of original PET (IV = 0.80 dl/g) is 10 kJ/m$^2$ while that of 13% EBA-GMA containing recycled PET (IV = 0.56 dl/g) already exceeds 40 kJ/m$^2$. For compounding, Labtech 26-44 (Labtech Engineering, Thailand) twin screw extruder with a screw diameter of 26 mm and an L/D ratio of 48 was used, with zone temperatures between 245-260°C and a rotor speed of 50 rpm. The extrusions were carried out in air atmosphere. After extrusion, the materials were granulated to cylindrical shape: $D$ = 2.0 ± 0.5 mm; $L$ = 3.5 ± 0.5 mm.

For the mechanical tests, dumbbell specimens according to ISO 527-2 1A were injection moulded from the compounded materials using a 50 MEtII (Mitsubishi, Japan) electric injection moulding machine. Zone temperatures varied from 255°C to 270°C, and mould temperature was 60°C. Injection speed was 90 mm/s, holding pressure was 50 MPa, and back pressure was 10 MPa. All the compounded materials were dried at

160°C for 4 hours before injection moulding.

#### 2.2.2. Characterisation methods

The moisture content of the PET granules was determined by a HydroTracer FLV (Aboni, Germany) type moisture meter. The apparatus measures the absolute water content; during heating the sample to 200°C, the evaporating gaseous water reacts with the calcium hydride reagent in the reactor of the instrument to form hydrogen, from the concentration of which, after compensated by the humidity of the air, the water content can be determined.

The Melt Flow Index (*MFI*) measurement was performed by LMI 4000 (Dynisco, USA) device with 260°C / 1.2 kg parameters.

IV measurements were carried out according to the ASTM D4603 standard; the IV was calculated by the Billmeyer equation. The IV values of the PET materials were determined using an RPV-1 (PSL Rheotek, USA) automatic solution viscometer. The measurements were done at 30°C in a 60/40 weight mixture of phenol/tetrachloroethane solvent with a concentration of 0.5 g/dl.

Scanning electron microscopic (SEM) images were obtained using EVO MA 10 instrument (Zeiss, Germany) at an accelerating voltage of 25 kV on specimens. For this, injection moulded specimens were cut, embedded in epoxy resin, polished, and after that, the embedded specimens were immersed in toluene (Molar Chemicals, Hungary) for 4 hours at room temperature to dissolve the EBA-GMA phases. For SEM analysis 5 nm gold coating was applied.

Izod impact tests were carried out by a 5113.10.01 type (Zwick, Germany) impact tester at room temperature. Pendulum energy was 5.4 J. Tests were performed according to ISO 179-1 standard using notched specimens.

Tensile strength and modulus were determined by an L3369 (Instron, USA) universal machine according to ISO 527-2 standard. Tensile modulus of elasticity was determined between 0.05% and 0.25% relative elongation at 1 mm/min crosshead speed, using a video extensometer. Tensile strength test was carried out at 10 mm/min crosshead speed.

The glass transition temperature of EBA-GMA was determined by a TSC II (Setaram, France) equipment using thermally stimulated depolarization current (TSDC) technique. This method is suitable for investigating molecular mobilities with high sensitivity thus well applicable to examine small relaxations in materials containing one or more components [37,38]. During all measurements, the sample was polarized at 0°C ($T_p$) with 300 V ($U_p$) polarization voltage for 5 minutes ($t_p$). Then a cooling step followed with a 10°C/min ($r_c$) cooling rate to the -80°C freezing temperature ($T_0$) while the electric field was still present. The holding time at $T_0$ was 1 minute ($t_0$) and the polarization was turned off in this step. In the next step, a 5°C/min heating rate was used to reach the final temperature ($T_f$ = 0°C) while the depolarization current was recorded in the function of the temperature.

The crystallinity of the samples was determined using a DSC131 EVO (Setaram, France) DSC device. The DSC measurements were performed in nitrogen atmosphere with a flow rate of 50 ml/min, heat-cool cycles were applied between 0-300°C, at 10°C/min heating and cooling rates. The weight of the examined samples was between 10-15 mg. Crystallinity percentage ($\chi_c$) of PET was calculated according to Eq. (1), where $\Delta H_m$ is the melting enthalpy, $\Delta H_{cc}$ is the cold crystallization enthalpy, $\Delta H_m^0$ is the melting enthalpy of a perfect PET crystal equal to 140.1 J/g [39] and $\Phi_{EBA\text{-}GMA}$ is the mass ratio of EBA-GMA additive.

$$\chi_c\ [\%] = \frac{\Delta H_m - \Delta H_{cc}}{\Delta H_m{}^0 (1 - \phi_{EBA-GMA})} \cdot 100\% \tag{1}$$

## 3. Results

### 3.1. Effect of moisture content on PET degradation during processing

The equilibrium moisture content of the used PET granules stored at 23 ±1°C / 50 ± 5% RH was measured to be 2200 ppm. The moisture uptake of PET granules, pre-dried at 160°C to equilibrium water content (27 ppm), when placed in a climatic chamber set to 23°C / 80% RH is shown in Fig. 2 as a function of logarithmically plotted time. Four Parameter Logistic (4PL) curves (Eq. 2) can be fitted to the measuring points ($R^2 = 0.997$):

$$MC\ (t) = MC_\infty \frac{MC_0 - MC_\infty}{\left[1 + \left(\frac{t}{t_{MC,50}}\right)^{C_{MC}}\right]}, \tag{2}$$

where *MC (t)* is the moisture content at a given time point; $MC_0$ = 30 ppm is the moisture content at zero time, $MC_\infty$ = 13360 ppm is the moisture content at theoretical infinite time, $t$ [min] is exposure time; $t_{MC,\ 50}$ = 87 272 min is the inflection point (i.e. the point on the S-shaped curve halfway between $MC_0$ and $MC_\infty$) and $C_{MC}$ = 0.47 is the Hill's slope of the curve (i.e. this is related to the steepness of the curve at point $t_{50}$).

It can be seen in Fig. 2 that after about one week (i.e. 10000 min) of exposure, the water uptake of the round PET granules reaches 3520 ppm. Samples were taken at six time points within this period; namely after 0, 2, 7, 24, 54 and 168 hours of exposure, and then these PET granules, differing in initial moisture content, were used in extrusion processes. It is noteworthy that the extrusions were carried out in air atmosphere. If oxygen would have been excluded, besides degradation due to thermal, hydrolytic and mechanical effects, chain extension accompanied with noticeable molecular weight increase would have also occurred [40]. The degree of degradation that occurred during processing was examined by performing MFI and IV measurements on the obtained extrudates.

In Table 1, the IV and MFI values of the PET grades, differing in initial moisture content ranging between 30 and 3520 ppm, are presented, as measured after melt extrusion using identical processing parameters. It can be seen that moisture content of 570 ppm already reduces the IV of extruded PET drastically, from 0.69 dl/g to 0.56 dl/g; and accordingly, a noticeable increase of the MFI (from 21 g/10 min to 40 g/10 min) can be measured. Such a degree of degradation results already in a significant property loss. The relationship between the two values can be described by Eq. (3) ($R^2 = 0.966$).

$$IV_{30°C} = -0.167 \cdot \ln\left(MFI_{260°C;1.2kg}\right) + 1.154\ dl/g \tag{3}$$

The change in the IV value of the PET after extrusion as a function of its initial moisture content is plotted in Fig. 3. An exponential relationship can be fitted to the data according to Eq. (4) ($R^2 = 0.968$). The shape of the resulting curve (Fig. 3) is in good agreement with the literature [13].

$$IV\ (MC) = 0.41\frac{dl}{g} + 0.28dl \Big/ g * e^{-8.38*10^{-4}*MC}, \tag{4}$$

where *MC* [ppm] is the initial moisture content.

Based on the obtained exponential relationship, it can be established that the rate of chain cleavage during processing is greatly enhanced by increasing moisture content.

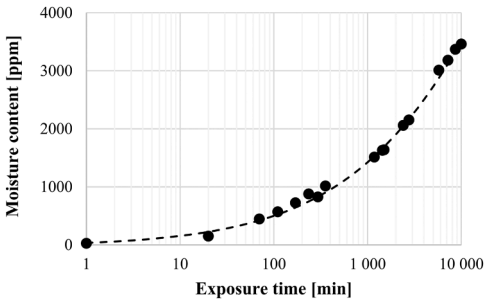


**Fig. 2.** Moisture uptake of PET granules at 23°C / 80% RH.

**Table 1**
IV and MFI values of PET grades after melt extrusion with increasing initial moisture content.

| Exposure time at 23°C / 80% RH [h] | Moisture content [ppm] | IV [g/dl] | MFI [g/10 min] |
|---|---|---|---|
| 0 | 30 | 0.69 | 21 |
| 2 | 570 | 0.56 | 40 |
| 7 | 970 | 0.53 | 47 |
| 24 | 1710 | 0.50 | 47 |
| 54 | 2310 | 0.46 | 58 |
| 168 | 3520 | 0.41 | 63 |

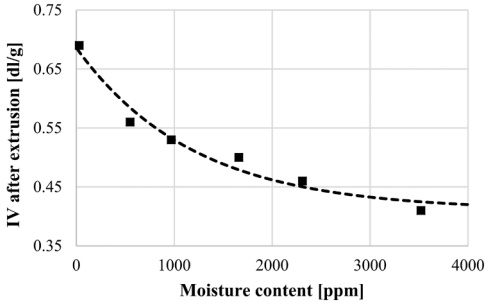


**Fig. 3.** Effect of initial moisture content on the IV value of extruded PET.

### 3.2. Mechanical properties of the toughened blends

In our previous research, a major effect of the molecular weight of the used PET grade was evinced on the toughening efficiency of the EBA-GMA type reactive terpolymer [27]. As a continuation of this research, in this study, the *in situ* hydrolytic degradation triggered evolution of compatibilisation reactions and elastomer crosslinking is investigated. For this purpose, six grades of PET, differing in initial moisture contents ranging between 30 and 3520 ppm, were used for melt blending with a constant 13% ratio of EBA-GMA. The static and dynamic mechanical performance of the blends obtained this way were examined while the related changes in the morphological, structural, and rheological properties were comprehensively explored.

Fig. 4 shows the change in notched Izod impact strength of the 13% EBA-GMA containing blends as a function of the initial moisture content of the used PET, also in comparison with the performance of the corresponding additive-free PET grades submitted to identical extrusion and subsequent injection moulding processes. In the examined range of moisture content (i.e. up to 3520 ppm), the impact strength of neat PET reduces closely linearly with moisture content, from 3.2 kJ/m$^2$ to 2.9 kJ/m$^2$. It can be seen that the impact strength of the PET/EBA-GMA blends is noticeably higher in the entire range of moisture content. In the initial range, the impact strength increases slightly, from 8 to 16 kJ/m$^2$. Around the initial moisture content of 1710 ppm, however, this value increases abruptly, and impact strength as high as 53 kJ/m$^2$ is

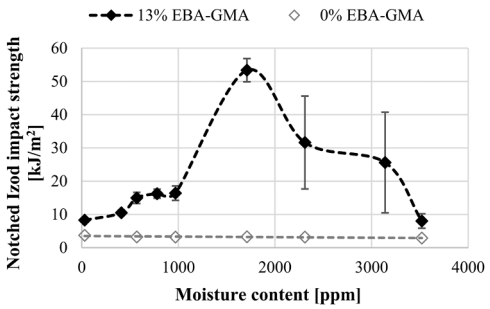


**Fig. 4.** Notched Izod impact strength of the PET/EBAGMA blends as a function of initial moisture content of the used PET.

reached, which means a 6-fold increase compared to the PET/EBA-GMA blend of identical chemical composition, but produced from completely dried PET, and a 16-fold increment compared to the additive-free PET of identical moisture content. At higher moisture contents (above 1710 ppm) of the used PET, a decrease in impact strength can be observed, which returns to the initial value of about 8 kJ/m$^2$ at a moisture content of 3520 ppm.

The quasi-static mechanical properties of the extruded and injection moulded materials were characterized by tensile testing. The tensile strength of the additive-free PET varies around 58-60 MPa independently of the moisture content (Fig. 5/a). In contrast, the tensile strength of the PET/EBA-GMA blends shows an increasing tendency up to the initial moisture content of 3140 ppm, where, compared to the fully dried blend, an 18% increase in tensile strength (from 34 to 40 MPa) was measured. At an initial moisture content of 3520 ppm, the tensile strength of the PET/EBA-GMA blend decreases to 38 MPa.

The Young modulus of neat and EBA-GMA containing PET does not change noticeably in the examined range of initial moisture content (Fig. 5/b). The terpolymer-free PET samples have higher stiffness with Young modulus values in the range of 2850-3100 MPa, while this value falls in the range of 1500-1700 MPa in the case of the blends.

The strain at break of the additive-free materials decreases exponentially as a function of moisture content. In the case of the blends, however, this value remains quasi constant at a value of 140% up to the initial moisture content of 3140 ppm, above which there is a significant drop in this characteristic. Using PET with an initial moisture content of 3530 ppm – similar to the tensile strength – the strain at break falls back noticeably, from 137% to 100% (Fig. 5/c). This value is, however, still noticeably higher than those of the terpolymer-free PET materials.

### 3.3. Morphology of the toughened blends

SEM images taken from the cross section of the blends after the selective dissolution of the EBA-GMA phase are shown in Fig. 6. It can be observed that the characteristic size of the rubber phase decreases continuously with the increasing initial moisture content of PET. At identical additive content, the refinement of the particle size distribution indicates improved interfacial compatibilisation [41]. The particle size of 50-100 μm formed at low (30-970 ppm) moisture content reduces to 5-20 μm at 1710 ppm and even to 1-5 μm when PET with an initial moisture content of 3520 ppm is used for melt blending. Also, with decreasing particle size as a function of initial moisture content of PET, the shape of the dispersed phase becomes more spherical, and the size of the dispersed particles becomes increasingly homogeneous.

### 3.4. Structure of the toughened blends

#### 3.4.1. Crystalline structure of PET

The crystalline characteristics of PET can influence the evolution of the mechanical properties of the polymer itself and its rubber toughened blends alike [35]. Therefore, investigation of the crystalline structure of PET is important to explore its potential relation to the changes in the perceived impact behaviour. The crystalline structure of the terpolymer-free and 13% EBA-GMA containing injection moulded specimens was examined by DSC method. Table 2 shows the cold crystallization enthalpy ($\Delta H_{cc}$) and temperature ($T_{cc}$), the crystal melting enthalpy ($\Delta H_m$) and temperature ($T_m$), determined from the first heating cycle, and the crystallization enthalpy ($\Delta H_c$) and temperature ($T_c$), derived from the cooling cycle of the DSC measurements, respectively. The calculated initial crystallinity is plotted in Fig. 7.

Rapid cooling during injection moulding resulted in highly amorphous structure, as indicated by the large cold crystallization enthalpies [42]. The cold crystallization temperature ($T_{cc}$) of PET decreases with increasing moisture content both in the case of the neat polymer and the PET/EBA-GMA blends. However, PET chains in the blends acquire enough energy to diffuse to the surface of PET crystals at lower

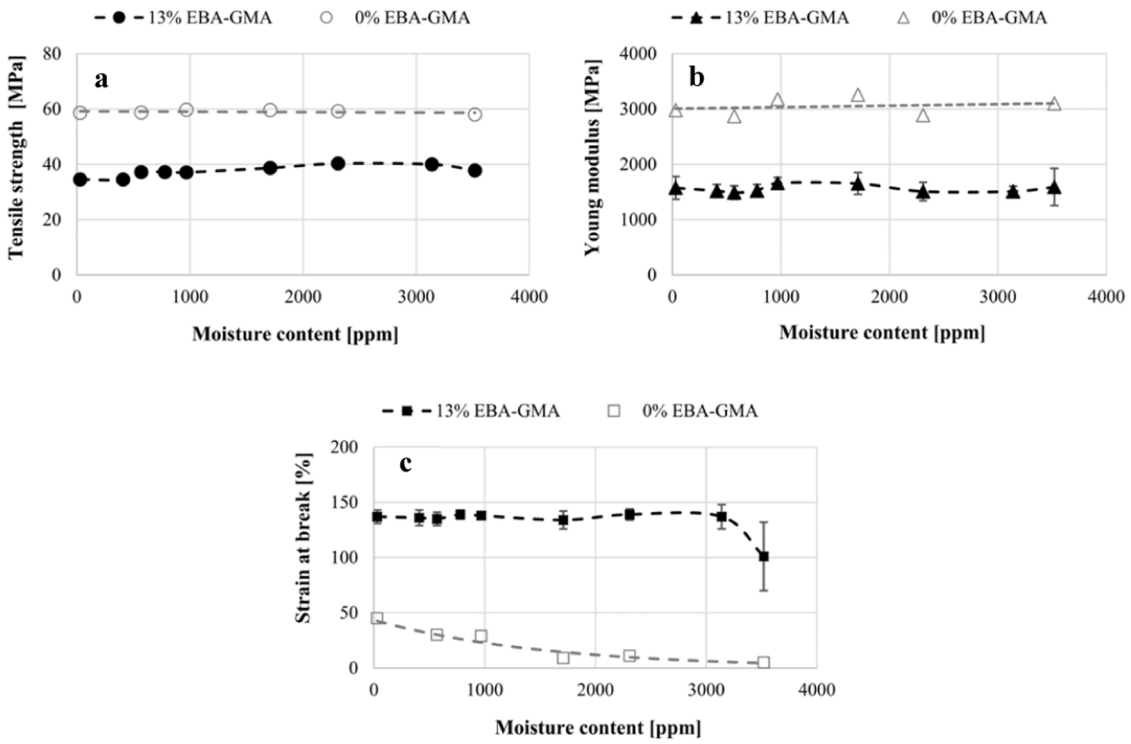


**Fig. 5.** Change of quasi-static mechanical properties of PET/EBA-GMA blends as a function of initial moisture content of PET (**a**: tensile strength; **b**: Young modulus; **c**: strain at break).

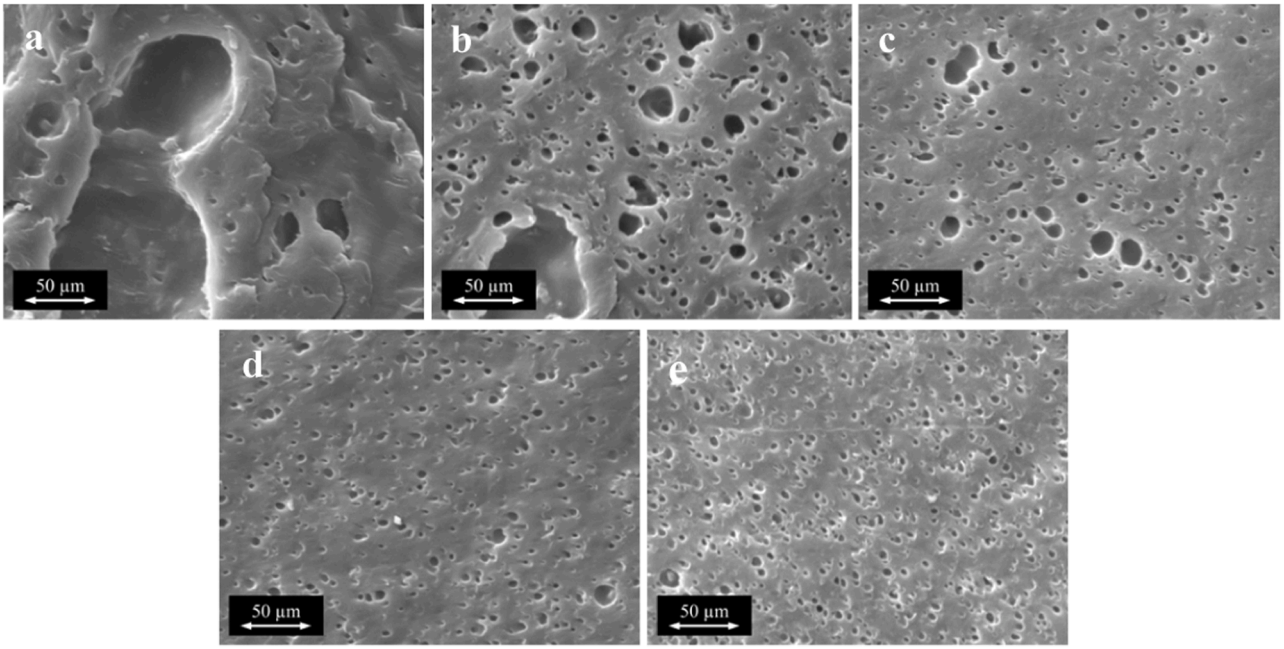


**Fig. 6.** SEM images of the polished crosssection of PET/EBA-GMA blends with constant EBA-GMA ratio but varying initial moisture content **a**: 30 ppm; **b**: 970 ppm; **c**: 1710 ppm; **d**: 2330 ppm; **e**: 3520 ppm.

temperatures during heating up, so $T_{cc}$ decreases compared to neat PET, especially in the case of blends with a low (< 2310 ppm) initial moisture content.

It can be observed in Fig. 7 that with increasing initial moisture content, the crystalline proportion increases by following a similar trend in both cases. It is therefore assumed that in both cases the increasing crystalline ratio is associated with the decreasing molecular weight of PET due to the increasing degree of hydrolytic degradation, which enhances the mobility of the chains and favors the ordering of the polymer segments with short chains [43]. These results are in agreement with the measurements of Badia et al. [44], where the IV value of the original PET was reduced to less than 0.5 dl/g by repeated extrusion steps, during which the crystalline proportion increased by 3%.

The crystallinity of PET is also affected by the terpolymer. It seems to decrease in the presence of the terpolymer, but increases as a result of interfacial layer modification. Nevertheless, $T_m$ shows an increase in the

**Table 2**
Results of DSC measurements.

| EBA-GMA content [%] | Moisture content [ppm] | $T_{cc}$ [°C] | $\Delta H_{cc}$ [J/g] | $T_m$ [°C] | $\Delta H_m$ [J/g] | $T_c$ [°C] | $\Delta H_c$ [J/g] |
|---|---|---|---|---|---|---|---|
| 0 | 30 | 134.1 | -25.6 | 252.9 | 36.7 | 189.9 | -35.3 |
| | 970 | 131.2 | -26.4 | 254.0 | 39.6 | 192.1 | -35.5 |
| | 1710 | 131.2 | -25.9 | 254.5 | 39.2 | 191.2 | -36.2 |
| | 2310 | 130.1 | -25.3 | 255.4 | 39.0 | 191.7 | -36.4 |
| | 3520 | 125.8 | -24.4 | 255.0 | 39.8 | 192.7 | -37.8 |
| 13 | 30 | 132.0 | -19.6 | 253.7 | 28.3 | 180.6 | -30.2 |
| | 970 | 126.4 | -17.1 | 254.4 | 29.9 | 181.9 | -31.0 |
| | 1710 | 125.6 | -18.4 | 254.7 | 32.9 | 182.7 | -31.6 |
| | 2310 | 125.6 | -20.2 | 255.4 | 36.0 | 184.6 | -32.2 |
| | 3520 | 122.1 | -21.3 | 255.5 | 36.0 | 190.4 | -33.2 |

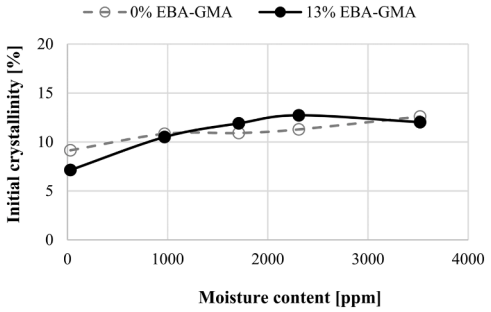


**Fig. 7.** Initial crystallinity of the injection moulded specimens with and without EBA-GMA at different moisture contents.

effect of moisture content (Table 2), and this value is slightly higher for the blends than for the additive-free materials. The higher $T_m$ value indicates larger crystallite size [45].

### 3.4.2. Molecular structure (crosslinking) of the rubber phase

The degree of crosslinking of the EBA-GMA terpolymer in the PET/EBA-GMA blends was assessed by accurate measurement of $T_g$ by TSDC method. This method is more sensitive than DSC to characterize the dispersed phase being present in a small proportion [46]. Fig. 8 shows that the $T_g$ of EBA-GMA shows a decreasing tendency as a function of the initial moisture content of PET used for blending. The $T_g$ values measured for the PET/EBA-GMA blends of initial moisture contents higher than 1710 ppm are below -50.0°C. It is noteworthy that these $T_g$ values are closely identical with the $T_g$ of the neat (uncrosslinked) EBA-GMA (-50.8 ± 0.2°C).

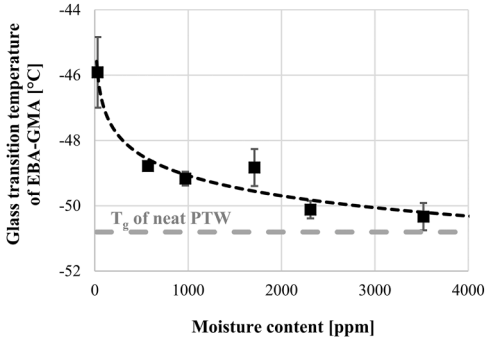


**Fig. 8.** Glass transition temperature of the rubbery phase of PET/EBA-GMA blends as a function of initial moisture content of the used PET.

### 3.5. Rheology of the toughened blends

In the case of the EBA-GMA containing blends, IV measurements could not be performed due to the changed solubility, so the viscosity of the blends was characterised only by their MFI value.

The MFI values of the PET/EBA-GMA blends were measured by using the same parameters as in the case of the terpolymer-free PET extrudates (Table 1). Under these conditions, an MFI value of 24 g / 10 min was determined for the EBA-GMA additive. It can be seen in Table 3, that the MFI values of the 13% EBA-GMA containing PET blends, in most cases, fall below this value.

In Fig. 9, the relative MFI values of 13% EBA/GMA containing blends to that of the corresponding additive-free PET are plotted as a function of moisture content. It can be seen that at lower inital moisture contents (<1000 ppm) the MFI values of the PET/EBA-GMA blends are only about one-twelfth of the those of the corresponding elastomer-free PET materials. The relative MFI values then start to increase from a moisture content of 1000 ppm and reach about 50% of the flowability of the additive-free PET at 3520 ppm.

## 4. Discussion

Our experimental results reveal that the initial moisture content of PET significantly influences the impact strength of PET/EBA-GMA blends prepared by extrusion. In the case of PET/EBA-GMA blends of 13% EBA-GMA content, a 6-fold increase in notched Izod impact strength was achieved only by setting the initial moisture content of the used PET granule to 1710 ppm, which seems to be around the optimal value in this respect. It is also noteworthy that without conditioning, the equilibrium moisture uptake (2200 ppm) of PET granules stored at 23 ± 1°C / 50 ± 5 % RH is very close to this optimum value.

The noticeable change in the notched impact resistance of PET/EBA-GMA blends as a function of the initial moisture content of PET is a consequence of the evolution of the compatibilisation and crosslinking reactions during processing according to the following explanation.

### 4.1. Low moisture content (< 1000 ppm) - significant terpolymer crosslinking

Without moisture, high molecular weight PET chains with fewer functional end groups and limited molecular mobility are present, which limit the reaction with the epoxide function of the reactive toughener. As a result, the EBA-GMA terpolymer becomes more susceptible to crosslinking, leading to a greater and less deformable dispersed phase, as found on the SEM images of the PET/EBA-GMA blend prepared by starting from fully dried PET granules (Fig. 6/a). At this minimal moisture content of 30 ppm, the dispersed rubber particles are large (50-100 μm). During failure, the formation of crazes is the dominant process, and a typical brittle fracture surface can be observed after impact testing (Fig. 10/a).

The presence of uncompatibilised elastomer restricts the movement of the PET molecular chains and hence decreases the crystallization temperature ($T_c$) of PET compared to additive-free PET, especially in the case of blends with a low initial moisture content, where the degree of

**Table 3**
MFI values of PET with 13% EBA-GMA content after melt-extrusion with increasing initial moisture content.

| Exposure time at 23°C / 80% RH [h] | Moisture content [ppm] | MFI [g/10 min] |
|---|---|---|
| 0 | 30 | 2 |
| 2 | 570 | 3 |
| 7 | 970 | 4 |
| 24 | 1710 | 8 |
| 54 | 2310 | 19 |
| 168 | 3520 | 31 |

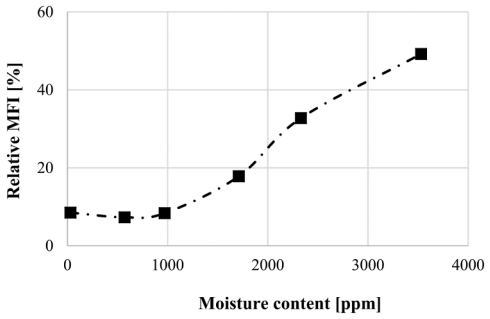


**Fig. 9.** Relative MFI of the blends to that of the corresponding additive-free PET as a function of initial moisture content.

compatibility is not yet high (Table 2). These conclusions are in agreement with the results of Zhang et al. [45] who also found restricted movement of PET molecules accompanied with decreased $T_c$ in the presence of SEBS or SEBS-g-MA, however, $T_c$ of PET in the compatibilised blends was found to be noticeably higher than that of PET in the uncompatibilised blend.

The degree of crosslinking of the EBA-GMA phase was monitored by examining the glass transition temperature of the elastomer. TSDC results revealed that crosslinking level of the PET/EBA-GMA blends is the highest when fully dried PET is used (Fig. 8).

The relative MFI value of PET / EBA-GMA blends (i.e. relative to that of the corresponding additive-free PET materials with the same initial moisture content) decreases to the greatest extent (by more than 90%) at low moisture contents (Fig. 9). This can also be explained by the presence of large, crosslinked rubber phases that reduce the flowability of the material [47,48].

### *4.2. Increased moisture content (1000– 3200 ppm) - effective compatibilisation*

SEM images (Fig. 6) show that the average size of the dispersed rubber phase decreases as a function of increasing initial moisture content in the system resulting in a smaller interparticle distance. When the ligament thickness drops below a critical value, the dispersed rubber particles form an infinitive interconnected network of stress volumes, causing the impact strength to increase exponentially. The critical ligament thickness is not a fixed value but depends on testing conditions and the molecular chain length of the matrix. At a moisture content of 1710 ppm, the average ligament thickness noticeably decreased compared to blends of lower initial moisture content (Fig. 6). The corresponding ductile fracture surface indicates a strong shear-yielding (Fig. 10/b), according to which this ligament thickness is already below the critical value, taking into account the molecular weight of the PET matrix.

The reduction in the size of the dispersed rubber phase is due to the increasingly efficient compatibilisation reaction between the shorter PET molecules, being increasingly reactive with reducing chain length, and EBA-GMA. During thermomechanical processing, the length of the PET chains decreases *in situ*, in proportion to the moisture content being present in the system, enabling the formation of an increasingly effective TEI layer which is of key importance in achieving increased impact strength at reduced terpolymer content [26]. Thus, our findings suggest that shorter PET molecular chains aid in compatibilisation, in contrast to previous assumptions that assumed increasing extent of crosslinking reactions when the PET molar mass is reduced [32]. As a result of enhanced compatibilisation, the distribution of the EBA-GMA phase in PET is refined.

Crystallization temperature ($T_c$) of PET in the PET/EBA-GMA blends was found to increase with increasing moisture content, approaching the $T_c$ of the elastomer-free PET, also indicating better compatibility (Table 2). This is because the reaction of PET with EBA-GMA promotes the enrichment of PET on the interface and the orderly arrangement of PET chains facilitates the crystallization process during cooling [45]. In parallel, with the improvement of the compatibility of PET with the dispersed EBA-GMA phase, the motion of PET chains became less restricted, which is revealed by the decreasing $T_{cc}$ values.

$T_g$ of the elastomer gradually decreases with increasing moisture content being present in the system (Fig. 8); at initial moisture contents above 1710 ppm even approaching that of the neat (uncrosslinked) terpolymer, indicating decreasing degree of crosslinking in the EBA-GMA phase. This result suggests more effective compatibilisation reactions for the blends which contain PET chains of reduced molecular weight, formed as a result of *in situ* hydrolytic degradation of the polyester during processing.

Since improved compatibilisation due to increasing moisture content results in a smaller dispersed particle size, which is less restrictive of flowability, the relative MFI value of the blends increases (Fig. 9).

### *4.3. High moisture content (> 3200 ppm) - effective compatibilisation, but insufficient molecular entanglement*

Above an initial moisture content of 1710 ppm, a decrease in impact strength of the PET/EBA-GMA blends can be observed, although the particle refinement of the dispersed rubber phase continues and thus the ligament thickness also decreases (at least up to the examined moisture content of 3520 ppm). At a moisture content of 3520 ppm, the distribution of EBA-GMA is the finest, with average particle size and ligament

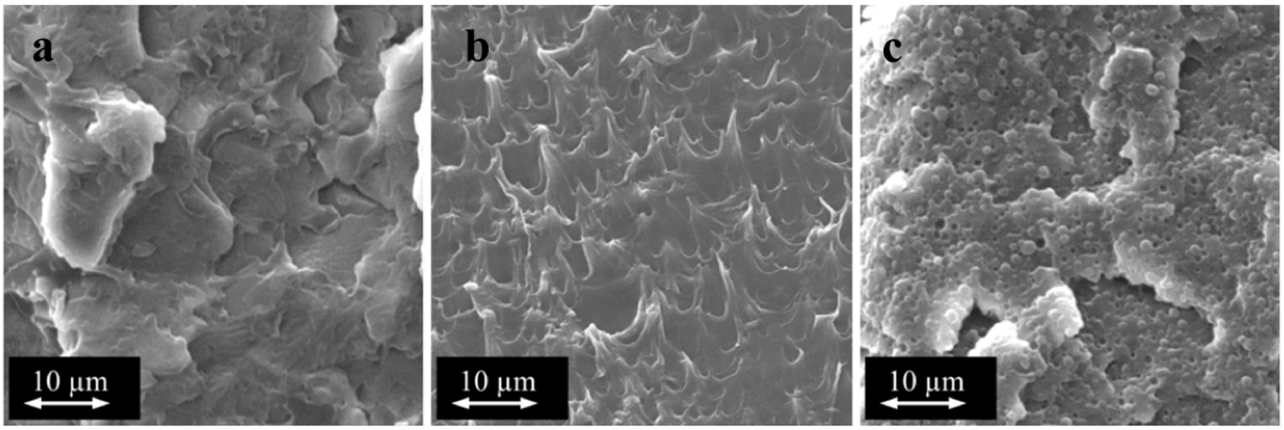


**Fig. 10.** SEM images of the fracture surface of PET/EBA-GMA blends with constant EBA-GMA ratio but varying initial moisture content **a**: 30 ppm; **b**: 1710 ppm; **c**: 3520 ppm.

thickness in the submicron range (Fig. 6/e). However, the fracture surface of these blends is brittle (Fig. 10/c) due to the significant reduction in the molecular chain length of high moisture containing PET, which causes the critical ligament thickness to shift. Furthermore, small rubber parts are less prone to cavitation, thus inhibiting the development of shear-yielding [49,47].

When during melt-processing too much water is present in the system, the molecular weight of PET decreases to such an extent that the molecular entanglement density falls below the critical value, so that a well-distributed and reactively bonded rubber cannot compensate for the brittle behavior of the matrix material. This decrease occurs at an IV of 0.42 dl/g, which is close to the limit of maintaining an entanglement network mentioned in the literature [22]. This is also supported by the reduction in the tensile strength and elongation at break of the blends manufactured from PET with high initial moisture content.

The shorter chains are easier to arrange into crystals. Brittleness may be also the consequence of the higher crystallinity. But the prominent impact strength cannot be traced back to crystallinity reasons, since the initial crystallinity of the terpolymer-free material was found to change in a similar way as that of the blends (Fig. 7).

$T_g$ of EBA-GMA further decreases above the moisture content of 1710 ppm, as measured by TSDC method (Fig. 8), which is related to the increasingly effective compatibilisation reactions and minimized crosslinking of the rubber phase.

## 5. Conclusions

Based on the present research study, a significant paradigm shift is proposed from the former view that moisture clearly reduces the impact strength of PET-based blends during processing.

It was found that the highly reactive short-chain fraction of PET, that is necessitated for creating the TEI and thus to achieve outstanding impact resistance at noticeably reduced terpolymer content, can be formed *in situ* during melt-processing through the accelerated hydrolytic degradation of PET in the presence of moisture. As a result, more than 6-fold increase of notched impact strength can be achieved only by "adding some water" to the system or by simply omitting the conventionally performed drying step. By utilizing this phenomenon, high impact resistant PET blends (notch Izod impact strength of 50 kJ/m$^2$) accompanied with prominent tensile characteristics (tensile strength: 40 MPa, Young modulus: 1500 MPa, strain at break: 140%) can be manufactured at noticeably (even by 50%) reduced elastomer content and simplified technology. The possibility of omitting the drying step means a further noticeable reduction of the production costs. This phenomenon can also give a driving force for the upgrading recycling of post-consumer PET.

The evinced outstanding increase of the notched impact resistance is found to be related to the intensified PET/EBA-GMA compatibilisation reactions and suppressed crosslinking of the rubber phase.

It is claimed that the efficiency of reactive modifiers in various polymeric systems can be effectively increased by the targeted utilisation of the increased reactivity of low-molecular-weight polymer fractions, whether from waste [27] or formed *in situ* during melt processing. The related PCT patent application is pending [50].

## CRediT authorship contribution statement

**Ferenc Ronkay:** Conceptualization, Methodology, Writing – original draft. **Béla Molnár:** Investigation, Methodology. **Edina Szabó:** Investigation. **György Marosi:** Supervision, Writing – review & editing. **Katalin Bocz:** Conceptualization, Methodology, Writing – original draft, Supervision.

## Declaration of Competing Interest

The authors declare the following financial interests/personal relationships, which may be considered as potential competing interests.

## Acknowledgments

The project was funded by the National Research, Development and Innovation Fund of Hungary in the frame of the 2018-1.3.1-VKE-2018-00017, 2019–1.3.1-KK-2019–00004 and GINOP_PLUSZ-2.1.1-21-2022-00041 projects. The research was funded by the Hungarian Scientific Research Fund, grant number FK128352. The research reported in this paper and carried out at the Budapest University of Technology and Economics has been supported by the National Research Development and Innovation Fund (TKP2020 Institution Excellence Subprogram, Grant No. BME-IE-NAT) based on the charter of bolster issued by the National Research Development and Innovation Office under the auspices of the Ministry for Innovation and Technology.

## References

[1] H. Wu, S. Lv, Y. He, J.P. Qu, The study of the thermomechanical degradation and mechanical properties of PET recycled by industrial-scale elongational processing, Polym. Test. 77 (2019), 105882, https://doi.org/10.1016/j.polymertesting.2019.04.029.
[2] F. Awaja, D. Pavel, Recycling of PET, Eur. Polym. J. 41 (2005) 1453–1477, https://doi.org/10.1016/j.eurpolymj.2005.02.005.
[3] F.P. la Mantia, M. Vinci, Recycling poly(ethyleneterephthalate), Polym. Degrad. Stab. 45 (1994) 121–125, https://doi.org/10.1016/0141-3910(94)90187-2.
[4] A.E. Schwarz, T.N. Ligthart, D. Godoi Bizarro, P. de Wild, B. Vreugdenhil, T. van Harmelen, Plastic recycling in a circular economy; determining environmental performance through an LCA matrix model approach, Waste Manage. 121 (2021) 331–342, https://doi.org/10.1016/j.wasman.2020.12.020.
[5] B.D. Vogt, K.K. Stokes, S.K. Kumar, Why is recycling of postconsumer plastics so challenging? ACS Appl. Polymer Mater. 3 (2021) 4325–4346, https://doi.org/10.1021/acsapm.1c00648.
[6] A.A. Karanastasis, V. Safin, L.M. Pitet, Bio-based upcycling of poly(ethylene terephthalate) waste for the preparation of high-performance thermoplastic copolyesters, Macromolecules 55 (2022) 1042–1049, https://doi.org/10.1021/acs.macromol.1c02338.
[7] J.M. Millican, S. Agarwal, Plastic pollution: a material problem? Macromolecules 54 (2021) 4455–4469, https://doi.org/10.1021/acs.macromol.0c02814.
[8] J.N. Hahladakis, E. Iacovidou, Closing the loop on plastic packaging materials: What is quality and how does it affect their circularity? Sci. Total Environ. 630 (2018) 1394–1400, https://doi.org/10.1016/j.scitotenv.2018.02.330.
[9] I. Antonopoulos, G. Faraca, D. Tonini, Recycling of post-consumer plastic packaging waste in the EU: recovery rates, material flows, and barriers, Waste Manage. (Oxford) 126 (2021) 694–705, https://doi.org/10.1016/j.wasman.2021.04.002.
[10] H. Zimmerman, N.T. Kim, Investigations on thermal and hydrolytic degradation of poly(ethylene terephthalate), Polym. Eng. Sci. 20 (1980) 680–683, https://doi.org/10.1002/pen.760201008.
[11] A. Pawlak, M. Pluta, J. Morawiec, A. Galeski, M. Pracella, Characterization of scrap poly(ethylene terephthalate), Eur. Polym. J. 36 (2000) 1875–1884, https://doi.org/10.1016/S0014-3057(99)00261-X.
[12] G. Giannotta, R. Po', N. Cardi, E. Tampellini, E. Occhiello, F. Garbassi, L. Nicolais, Processing effects on poly(ethylene terephthalate) from bottle scraps, Polym. Eng. Sci. 34 (1994) 1219–1223, https://doi.org/10.1002/pen.760341508.
[13] B. Molnar, F. Ronkay, Investigation of Morphology of Recycled PET by Modulated DSC, 2017, https://doi.org/10.4028/www.scientific.net/MSF.885.263.
[14] S. Al-AbdulRazzak, S.A. Jabarin, Processing characteristics of poly(ethylene terephthalate): hydrolytic and thermal degradation, Polym. Int. 51 (2002) 164–173, https://doi.org/10.1002/pi.813.
[15] E. Pirzadeh, A. Zadhoush, M. Haghighat, Hydrolytic and thermal degradation of PET fibers and PET granule: the effects of crystallization, temperature, and humidity, J. Appl. Polym. Sci. 106 (2007) 1544–1549, https://doi.org/10.1002/app.26788.
[16] N. Torres, J.J. Robin, B. Boutevin, Study of thermal and mechanical properties of virgin and recycled poly(ethylene terephthalate) before and after injection molding, Eur. Polym. J. 36 (2000) 2075–2080, https://doi.org/10.1016/S0014-3057(99)00301-8.
[17] S. Wu, Chain structure, phase morphology, and toughness relationships in polymers and blends, Polym. Eng. Sci. 30 (1990) 753–761, https://doi.org/10.1002/pen.760301302.
[18] H. Kanai, V. Sullivan, A. Auerbach, Impact modification of engineering thermoplastics, J. Appl. Polym. Sci. 53 (1994) 527–541, https://doi.org/10.1002/app.1994.070530507.
[19] N. Heymans, A novel look at models for polymer entanglement, Macromolecules 33 (2000) 4226–4234, https://doi.org/10.1021/ma9911849.
[20] J. Bicerano, Prediction of Polymer Properties, CRC Press, 2002. https://books.google.hu/books?id=5L1USsiq6KcC.
[21] T. Araki, M. Shibayama, Q. Tran-Cong, Structure and Properties of Multiphase Polymeric Materials, Taylor & Francis, 1998. https://books.google.hu/books?id=HDrA7300OZwC.

[22] J.M. Martínez, J.I. Eguiazábal, J. Nazábal, Influence of reprocessing and molecular weight on the properties of poly(ethylene terephthalate), J. Macromol. Sci. Part B 34 (1995) 171–176, https://doi.org/10.1080/00222349508219495.
[23] H. Wu, S. Lv, Y. He, J.-P. Qu, The study of the thermomechanical degradation and mechanical properties of PET recycled by industrial-scale elongational processing, Polym. Test. 77 (2019), 105882, https://doi.org/10.1016/j.polymertesting.2019.04.029.
[24] W. Loyens, G. Groeninckx, Deformation mechanisms in rubber toughened semicrystalline polyethylene terephthalate, Polymer 44 (2003) 4929–4941, https://doi.org/10.1016/S0032-3861(03)00478-6.
[25] W. Loyens, G. Groeninckx, Ultimate mechanical properties of rubber toughened semicrystalline PET at room temperature, Polymer 43 (2002) 5679–5691, https://doi.org/10.1016/S0032-3861(02)00472-X.
[26] I. Kelnar, V. Sukhanov, J. Rotrekl, L. Kapralkova, Toughening of recycled poly (ethylene terephthalate) with clay-compatibilized rubber phase, J. Appl. Polym. Sci. 116 (2010) 3621–3628, https://doi.org/10.1002/app.31905.
[27] K. Bocz, F. Ronkay, K.E. Decsov, B. Molnár, G. Marosi, Application of low-grade recyclate to enhance reactive toughening of poly(ethylene terephthalate), Polym. Degrad. Stab. 185 (2021), 109505, https://doi.org/10.1016/j.polymdegradstab.2021.109505.
[28] H. Cheng, M. Tian, L. Zhang, Toughening of recycled poly(ethylene terephthalate)/glass fiber blends with ethylene–butyl acrylate–glycidyl methacrylate copolymer and maleic anhydride grafted polyethylene–octene rubber, J. Appl. Polym. Sci. 109 (2008) 2795–2801, https://doi.org/10.1002/app.27564.
[29] M. Kaci, A. Benhamida, S. Cimmino, C. Silvestre, C. Carfagna, Waste and virgin LDPE/PET blends compatibilized with an ethylene-butyl acrylate-glycidyl methacrylate (EBAGMA) terpolymer, 1 morphology and mechanical properties, Macromol. Mater. Eng. 290 (2005) 987–995, https://doi.org/10.1002/mame.200500217.
[30] W.G. Perkins, Polymer toughness and impact resistance, Polym. Eng. Sci. 39 (1999) 2445–2460, https://doi.org/10.1002/pen.11632.
[31] A. Ghosh, Performance modifying techniques for recycled thermoplastics, Resour. Conserv. Recycl. 175 (2021), 105887, https://doi.org/10.1016/j.resconrec.2021.105887.
[32] S. Wu, Control of intrinsic brittleness and toughness of polymers and blends by chemical structure: a review, Polym. Int. 29 (1992) 229–247, https://doi.org/10.1002/pi.4990290313.
[33] Y. Qu, C. Rong, X. Ling, J. Wu, Y. Chen, H. Wang, Y. Li, Role of interfacial postreaction during thermal treatment: toward a better understanding of the toughness of PLLA/Reactive elastomer blends, Macromolecules 55 (2022) 1321–1331, https://doi.org/10.1021/acs.macromol.1c02273.
[34] M. Wang, X. Liang, H. Wu, L. Huang, G. Jin, Super toughed poly (lactic acid)/poly (ethylene vinyl acetate) blends compatibilized by ethylene-methyl acrylate-glycidyl methacrylate copolymer, Polym. Degrad. Stab. 193 (2021), 109705, https://doi.org/10.1016/j.polymdegradstab.2021.109705.
[35] W. Loyens, G. Groeninckx, Rubber toughened semicrystalline PET: influence of the matrix properties and test temperature, Polymer 44 (2003) 123–136, https://doi.org/10.1016/S0032-3861(02)00743-7.
[36] F. Ronkay, B. Molnár, D. Nagy, G. Szarka, B. Iván, F. Kristály, V. Mertinger, K. Bocz, Melting temperature versus crystallinity: new way for identification and analysis of multiple endotherms of poly(ethylene terephthalate), J. Polym. Res. 27 (2020) 372, https://doi.org/10.1007/s10965-020-02327-7.
[37] R.A. Shmeis, Z. Wang, S.L. Krill, A mechanistic investigation of an amorphous pharmaceutical and its solid dispersions, Part I: A comparative analysis by thermally stimulated depolarization current and differential scanning calorimetry, Pharm. Res. 21 (2004) 2025–2030, https://doi.org/10.1023/B:PHAM.0000048193.94922.09.
[38] J.S. Sedita, J.M. O'Reilly, A thermally stimulated depolarization current study of polymers in the glass transition region, Polym. Eng. Sci. 41 (2001) 15–22, https://doi.org/10.1002/pen.10704.
[39] J.D. Badia, E. Strömberg, S. Karlsson, A. Ribes-Greus, The role of crystalline, mobile amorphous and rigid amorphous fractions in the performance of recycled poly (ethylene terephthalate) (PET), Polym. Degrad. Stab. 97 (2012) 98–107, https://doi.org/10.1016/j.polymdegradstab.2011.10.008.
[40] M. Paci, F.P. la Mantia, Competition between degradation and chain extension during processing of reclaimed poly(ethylene terephthalate), Polym. Degrad. Stab. 61 (1998) 417–420, https://doi.org/10.1016/S0141-3910(97)00227-9.
[41] E. Jia, S. Zhao, Y. Shangguan, Q. Zheng, A facile fabrication of polypropylene composites with excellent low-temperature toughness through tuning interfacial area between matrix and rubber dispersion by silica nanoparticles located at the interface, Compos. Sci. Technol. 184 (2019), https://doi.org/10.1016/j.compscitech.2019.107846.
[42] H.J. Um, Y.T. Hwang, K.H. Choi, H.S. Kim, Effect of crystallinity on the mechanical behavior of carbon fiber reinforced polyethylene-terephthalate (CF/PET) composites considering temperature conditions, Compos. Sci. Technol. 207 (2021), https://doi.org/10.1016/j.compscitech.2021.108745.
[43] A. Ruvolo-Filho, P.S. Curti, PET recycled and processed from flakes with different amount of water uptake: characterization by DSC, TG, and FTIR-ATR, J. Mater. Sci. 43 (2008) 1406–1420, https://doi.org/10.1007/s10853-007-2282-6.
[44] J.D. Badia, E. Strömberg, S. Karlsson, A. Ribes-Greus, The role of crystalline, mobile amorphous rigid amorphous fractions in the performance of recycled poly (ethylene terephthalate) (PET), Polym. Degrad. Stab. 97 (2012) 98–107, https://doi.org/10.1016/j.polymdegradstab.2011.10.008.
[45] Y. Zhang, H. Zhang, L. Ni, Q. Zhou, W. Guo, C. Wu, Crystallization and mechanical properties of recycled poly(ethylene terephthalate) toughened by styrene-ethylene/butylenes-styrene elastomer, J. Polym. Environ. 18 (2010) 647–653, https://doi.org/10.1007/s10924-010-0223-y.
[46] J.J.M. Ramos, H.P. Diogo, The determination of the glass transition temperature by thermally stimulated depolarization currents. Comparison with the performance of other techniques, Phase Transitions 90 (2017) 1061–1078, https://doi.org/10.1080/01411594.2017.1320715.
[47] H. Liu, F. Chen, B. Liu, G. Estep, J. Zhang, Super toughened poly(lactic acid) ternary blends by simultaneous dynamic vulcanization and interfacial compatibilization, Macromolecules 43 (2010) 6058–6066, https://doi.org/10.1021/ma101108g.
[48] X. Hu, Y. Wang, J. Yu, J. Zhu, Z. Hu, Super toughened poly(trimethylene terephthalate) composite using flowable crosslink elastomer blend, Polym. Eng. Sci. 58 (2018) 2039–2046, https://doi.org/10.1002/pen.24815.
[49] J. Wang, X. Zhang, L. Jiang, J. Qiao, Advances in toughened polymer materials by structured rubber particles, Prog. Polym. Sci. 98 (2019), 101160, https://doi.org/10.1016/j.progpolymsci.2019.101160.
[50] Á. Mihályfi, L. Helmajer, Z. Lovas, K. Bordácsné Bocz, F. Ronkay, B. Molnár, G. Marosi, Thermoplastic Polyester and its Production, 2021. PCT/HU2021/050064, WO 2022/112807.